Essential oil-based nano-emulsions: Effect of different surfactants, sonication and plant species on physicochemical characteristics

Essential oil-based nano-emulsions: effect of different surfactants, sonication and plant species on physicochemical characteristics

Orlando Campolo[1], Giulia Giunti[1], Maryne Laigle[2], Thomas Michel[2*], Vincenzo Palmeri[1]

[1]Department of Agriculture, University Mediterranea of Reggio Calabria, Loc. Feo di Vito, 89122, Reggio Calabria, Italy

[2]Université Côte d'Azur, CNRS, Institut de Chimie de Nice UMR 7272, 06108 Nice, France

[*]Corresponding Author: Thomas.MICHEL@univ-cotedazur.fr

Abstract

Essential oils (EOs) are promising active ingredients for biopesticides, although their use in field conditions is limited by several criticisms concerning their high volatility and degradability. To overcome these negative qualities, EOs can be encapsulated inside nanostructures (i.e. nanoparticles and nano-emulsions), which can guarantee the preservation of the insecticidal properties.

In the current study, oil in water (O/W) nano-emulsions of seven commercial EOs (15% anise, artemisia, fennel, lavender, peppermint, rosemary, sage) were developed using different non-ionic surfactants and formulation processes, to identify the best possible surfactant/process to produce stable nano-formulations. The EOs were firstly examined by gas-chromatography analyses to identify their chemical constituents. Sage, rosemary, peppermint, lavender and artemisia EOs were characterized by high percentage (up to 50%) of oxygenated monoterpenes, while fennel and anise EOs are mainly constituted by phenylpropenes (e.g. anethol). Then, nano-emulsions were developed via the self-emulsifying process alone or in combination with sonication, using four surfactants with different Hydrophilic Lipophilic Balance (HLB) index (5% Tween 20, Tween 80, Span 20 or Span 80). The physical characteristics (droplet size and surface charge) of nano-emulsions were analyzed through dynamic light-scattering technique.

Sonicated nano-formulations presented smaller and more homogeneous size of the micelles than the non-sonicated ones, resulting in more stable nano-emulsions. Furthermore, usually emulsions produced using Tween 80 as surfactant gave the best results in terms of droplet size and polydispersity index values. Therefore, Tween 80 sonicated nano-emulsions were examined during a storage period of 28 weeks to determine their stability over time and possible alteration of their physical characteristics. Results suggest that these nano-formulations had a good stability over time, since relatively small increases in PDI and size values were recorded. Formulation stability is a key issue for consideration in proposing botanical biopesticides for agricultural applications and our study projects the first step for the introduction of EO-based nano-emulsions into operative conditions.

Key words: Bioinsecticide formulation, Botanicals, Dynamic Light Scattering, Essential oil, Non-ionic surfactant.

1. Introduction

Essential Oils (EOs) are hydrophobic natural material containing secondary metabolites (i.e. monoterpene, sesquiterpene and phenylpropene). They are mainly produced by higher plants, especially aromatic ones (over 17000 species) (Asbahani et al., 2015). To be defined as EOs, the matrices must be obtained by hydrodistillation, steam distillation, dry distillation or by mechanical extraction from plant organs (Do et al., 2015). The historical sources of EOs originates in the Middle Ages from Arabs, who first developed the extraction techniques for these natural substances (i.e. steam and hydro-distillation) (Burger et al., 2019). EOs are synthesized by endocrine and/or exocrine plant glands, as well as epidermal cells (Svoboda and Greenaway, 2003), and can be stored in all plant organs such as flowers, leaves, roots, bark or seeds. EOs play a key role in plant defense and they can be produced in response to abiotic and biotic stress, but they can additionally serve as attractive allelochemicals for pollinators and other beneficial insects (Regnault-Roger et al., 2012). EOs have been widely employed in the traditional pharmacopeia and as food preservers due to their antimicrobial properties (Bakkali et al., 2008). Today, their use is constantly increasing because of the strong demand for natural ingredients in many sectors (e.g. cosmetic, flavor and fragrance industries).

Aside from antiseptic properties, in the last decades many studies evaluated the insecticidal activity of EOs against field crop pests (Isman et al., 2018), stored product pests (Campolo et al., 2018) and insect vectors (Baskar et al., 2018; Benelli, 2015; Pavela, 2015), highlighting great perspectives for the development of EO-based biopesticides. Pest control is crucial to ensure crop production, but the indiscriminate use of synthetic pesticides can cause several problems related to the environmental and human health (Pavela and Benelli, 2016). In this scenario, among the alternative tools to control insect pests, botanical-based pesticides are of major interest. Nevertheless, to date, few commercial products containing EOs as active components are commercially available, and limited efforts have been made to evaluate their efficacy in operative conditions. Most of the published studies focused on the screening of EO toxicity against target organisms in laboratory conditions, while sublethal effects and the impact on non-target organisms have been rarely studied (Isman and Grieneisen, 2014).

The main causes of the low conversion of laboratory studies into practical applications can be identified with a series of problematics related to some physicochemical characteristics of these substances (Pavela and Benelli, 2016). First, EOs are lipophilic liquids and they are generally poorly soluble in water, impairing an easy distribution in field conditions. Second, many EOs are known to be phytotoxic, in fact they could be used for weed control (Karalija et al., 2020). Thus, their direct application on crops may cause severe plant desiccation and yield loses (De Almeida et al., 2010; Ibáñez and Blázquez, 2020). Third, the constituents of EOs are volatile and highly degradable (i.e. they

can be thermolabile, oxidizable or hydrolysable) (Pavela and Benelli, 2016). The biodegradability of the EOs can be considered positive for the absence of residues on the products and in the environment, but the low persistence of pure EOs could reduce their efficacy against insect pests. The interest on the design of persistent EO-based formulations with insecticidal properties is rising, although researches are still at an early stage.

The increasing number of publications about the application of nanotechnology in agriculture highlights the opportunity to extend these techniques to bio-pesticides (He et al., 2019). The use of nano-encapsulation processes may guarantee the stability over time of the active ingredients, as well as their constant release, decreasing the adverse effects on plant tissues. Encapsulation processes require that the bioactive components are coated inside a matrix (i.e. a synthetic or natural polymer), which isolates the active ingredients from the external environment (Rodríguez et al., 2016). Several nano-encapsulation methods have been developed, but encapsulations inside nanoparticles or into nano-emulsions seem to be the most adequate and promising (Campolo et al., 2017; Giunti et al., 2019). Apart from the increased stability of the active components, nano-encapsulation ensures a good dispersibility/solubility in water.

Nano-emulsions are defined as kinetically stable systems, whose droplets usually present a size range from 50 to 200 nm (Tadros et al., 2004) . Thus, nano-emulsions presents a long-term physical stability, with no visible flocculation or coalescence for long periods, which is a distinctive characteristic of these nanomaterials. The long-term stability of nano-emulsions can be attribute to the impact of steric stabilization happening when using non-ionic surfactants or polymers (Tadros et al., 2004). Nano-emulsions present further advantages, like the lower quantity of surfactants required compared to micro-emulsions, the uniform surface coating and the good wetting, spreading and penetration ability (Bouchemal et al., 2004). Furthermore, the nano-metrical size of these systems can improve the efficacy of the active components. Nevertheless, the formulation of stable EO-based nano-emulsions can be dependent on the EO/surfactant combination and/or their ratio, and it can require high energy inputs, such as sonication. Usually, sonication and high amount of surfactant make the nano-emulsion's droplet size decrease; however, non-ionic surfactants are known to cause phytotoxicity themselves (Hess and Foy, 2000; Hurtt and Hodgson, 1987; Liu, 2004) or to increase the phytotoxic effect of some commercial herbicides (Liu, 2004; Mirgorodskaya et al., 2020; Niedobová et al., 2019; O'Donovan et al., 1985).

In the current research, we investigated, the role of different ingredients (i.e. EOs and non-ionic surfactants) and approaches (i.e. self-emulsification and sonication) on the EOs-based nano emulsion outcomes in terms of stability, droplet dimension, droplet homogeneity and surface charge. Different surfactants and EOs were tested and the

stability of the best formulations were evaluated over time. All the EOs as well as the developed nano-emulsions were chemical and physical characterised. The main objective of the experiments was to develop EO nano-delivery systems containing a high amount of essential oil (i.e. 15%) through a high oil:surfactant ratio (i.e. 3:1).

2. Materials and methods

2.1 Essential oils and chemical material

Anise (*Pimpinella anisum*), artemisia (*Artemisia vulgaris*), fennel (*Foeniculum vulgare*), lavender (*Lavandula angustifolia*), peppermint (*Mentha x piperita*), rosemary (*Rosmarinus officinalis*) and sage (*Salvia officinalis*) essential oils were obtained from Esperis s.p.a (Milan, Italy). Each EO was diluted at 80 mg/ml with pentane distilled before gas-chromatography analysis. Chemicals such as pentane, Tween 20, Tween 80, Span 20 and Span 80 were obtained from Sigma Aldrich (Milan, Italy).

2.2 Essential oils chemical characterization

2.2.1 Gas Chromatography analyses

GC/FID analysis.

The GC/FID analyses were performed using an Agilent 6890N gas chromatograph equipped with a flame-ionization detector (FID), an electronic pressure control (EPC) SSL injector (Agilent Technologies, J&W Scientific Products, Palo Alto, CA, USA), and an apolar HP-1 capillary column (100% polymethylsiloxane; 0.2mm x 50m; film thickness, 0.33 µm). The oven temperature was programmed rising from 40 °C to 200 °C at 2 °C/minute, then increased to 270 °C at 20 °C/minute and, finally, held isothermally at 270 °C for 20 minutes. Injector temperature was set at 220 °C and the detector temperature at 280 °C. Split ratio was 1/100 and injection volume 1 µL. Samples were injected in triplicate for quantitation.

GC-MS analysis.

The GC-MS analyses were carried out with a gas chromatograph model Agilent 6890 (Palo Alto, CA) equipped with a mass selective detector MSD5975B (Agilent) and a multifunction automatic sampler (Combi-Pal, CTC Analytics, Zwingen, Swiss) using an HP-1 MS capillary column (100 % polymethylsiloxane; 0.2 mm x 50 m; film thickness, 0.33 µm). The oven temperature was programmed rising from 40 °C to 200 °C at 2 °C/minute, from 200 to 270 °C at 20 °C/minute and kept isothermally at 270 °C for 20 minutes. Carrier gas was Helium (constant flow: 1 ml/minute); ionization voltage, 70 eV; scan time, 1 second; mass range, 40–300 amu. Split ratio was 1/100, injector temperature 250 °C with an injection volume of 1 µL.

2.2.2 Identification of volatile compounds

Compounds were identified by comparison of their mass spectra with existing mass-spectral libraries (Flora97, Lca98, NIST02) and of their linear retention index with those reported in the literature (NIST, Adams (2017)). Linear retention indices (LRI) were determined by performing GC-MS on a set of known alkanes (C5–C20) whose LRI times were used to calculate the LRI of the volatile compounds found in samples according to the definition of Van den Dool and Kratz.

2.3 Nano-emulsion formulation and characterization

All the nano-emulsions were prepared following Giunti et al. (2018), with modifications. Specifically, the nano-emulsions were obtained using the spontaneous emulsification process, which can naturally occur when an organic phase and an aqueous phase are mixed, followed by sonication. To evaluate the effect of surfactants on the droplet size and stability of the EO-based emulsions Span 80, Span 20, Tween 80, and Tween 20 with an hydrophilic-lipophilic balance value (HLB) of, 4.3, 6.7, 15.0 and 16.7 respectively were used for the nano-emulsion formulation. The process consisted in mixing using a magnetic stirrer (30 min at 8000 RPM) the surfactant (5% w:w) with the essential oil (15% w:w). Then, double-distilled water (80%) was dropwise (1 mL * min^{-1}) added to this mixture and then stirred for 60 min to attain a homogeneous emulsified phase. Furthermore, double-distilled water solutions containing each surfactant alone (5% w:w) were prepared and used as control for the subsequent analyses.

We hypothesized that the combination of self-emulsifying process and sonication may play a key role in the nano-emulsion stability and droplets' size. To evaluate the effect of the sonication process on the stability and physical parameters, the previously developed emulsions were sonicated for 5 min using an UP200ST ultrasonic immersion

homogenizer (Hielsher©, Teltow, Germany) at 100W power (frequency: 26 kHz). To avoid EOs degradation due to the heat generated by the sonicator, the process was carried out in an ice bath. The choice to use a high oil:surfactant ratio (i.e. 3:1) was based on preliminary tests that showed a phytotoxicity of the nano-formulations proportional to the amount of surfactant used.

The physical characteristics of the essential oil-based nano-emulsions were analysed by a Dynamic Light Scattering (DLS) instrument (Zetasizer Nano, Malvern). These qualitative analyses assessed the droplet surface charge at 25 °C, indicated by the zeta potential (ζ) values (electro-phoretic mobility of emulsions), and the droplets dimension, expressed in terms of Z-average size (Dz) and polydispersity index (PDI), of the tested formulations. To avoid multiple scattering effects 0.5 mL of every nano-emulsion were diluted in 100 mL of double-distilled water and aliquots (1 mL for Dz and 0.75 mL for ζ-potential) of the diluted emulsions were analysed. These physical characteristics are useful to determine the quality of the developed nano-emulsions and to predict the stability over time of the formulations. Low Z-average sizes (<200 nm) ensure that nano-metric droplets are obtained; it is commonly acknowledged that to smaller droplet sizes correspond better nano-emulsions. Similarly, nano-emulsions with PDI values close to zero are preferred; actually, low PDI values are characteristic of highly homogeneous nano-emulsions, which are less prone to Ostwald ripening destabilization phenomenon than non-homogeneous ones (Anarjan et al., 2014).. Droplet surface charge (ζ-potential) can play a role stabilizing the nano-emulsion by electrostatic repulsion (Müller et al., 2001; Tadros et al., 2004); however, using non-polar surfactants, stability is mainly attributable to steric stabilisation over electrostatic one, hence ζ-potential is not considered a primary parameter in the selection of optimal formulation. Nevertheless, drastic changes over time in all the described parameters can be alerts of the emulsion instability. Therefore, the physical characteristics of the best EO-based nano-emulsions were measured during the 1st, 2nd, 4th, 14th and 28th week of storage inside stainless steel bottles (1.2 L) at controlled conditions (T= 25 ± 1°C; RH= 50 ± 5%), to check for significant changes.

For each sample, three replicates of fourteen cycles were provided. Three samples were analysed as replicates for every tested parameter.

2.4 Statistical analysis

Dependent variables [Z-average size (Dz), the polydispersity index (PDI) and the zeta potential (ζ)] were subjected to non-parametric Mann Whitney (U) and Kruskal–Wallis (H) tests since the ANOVA assumption (homogeneity and normality of variance across the groups) were violated even after data transformation. To evaluate possible association

existing between two continuous variables (i.e. droplet size and PDI), the data were subjected to Pearson's correlation. All statistical analyses were conducted using IBM SPSS 19 statistical software.

3. Results

3.1 Essential oil composition

All the EOs were analyzed by mean of GC-MS and GC/FID. **Table S1 to S7** detailed components identified representing 90.77–98. 53% of the oils from different plant species. Sage, rosemary, peppermint, lavender and artemisia EOs were characterized by high percentage (up to 50%) of oxygenated monoterpenes, while fennel and anise EOs are mainly constituted by phenylpropenes (**Figure 1**). Sage, rosemary and fennel EOs also contain significant amount of hydrocarbon monoterpenes (between 27.68 % and 41.37 %). The most abundant compounds were eucalyptol (52.58 ± 0.1 %) in rosemary EO; menthol (38.63 ± 0.05 %) in peppermint EO; linalol (38.13 ± 0.1 %) along with linlayl acetate (33.42 ± 0.1 %) in lavender EO; (E)-anethol in fennel (40.58 ± 0.1 %) and anise (86.54 ± 0.2 %); EOs. Sage and rosemary EOs were characterized by mix of compounds including α-pinene, eucalyptol, α-thujone, β-thujone and camphor (**Table S1 and S5**).

3.2 Effect of surfactant and sonication on physical characteristics of nano-emulsions

Droplet size, PDI and ζ-potential were checked for all the developed nano-emulsions to determine the optimal formulation (**Table S8**). Statistical analyses aimed to highlight possible common trends across all the tested EOs and to select the best formulation process (i.e. sonication/no sonication) and composition (i.e. surfactant). Overall, the sonication and the surfactant seem to be the most important variables affecting the physical characteristics of the nano-emulsions. Sonication played a key role to reduce the droplet size and the PDI ($U_{1,\ 154}$=923.00; P<0.01 - $U_{1,\ 154}$=561.00; P<0.01) regardless the surfactant and the EO used to develop the nano-emulsions. Conversely, the sonication process did not affect the ζ-potential values ($U_{1,\ 154}$=3318; P = 0.328). The different surfactants influenced all the measured parameters (Size: $H_{3,152}$=54.16; P<0.01 – PDI: $H_{3,152}$=25.64; P<0.01 – ζ-potential: $H_{3,152}$=89.44; P<0.01). The formulations developed using the different EOs highlighted statistical differences in the PDI ($H_{6,149}$=18.45; P<0.01), whereas non statistical differences were registered for the ζ-potential values ($H_{6,149}$=4.60; P>0.59) and the droplet size ($H_{6,149}$=5.70; P>0.46).

In terms of stability, many of non-sonicated emulsions showed a separation into two different phases just 24 hours after the production (**Figure 2**). Only the emulsions made with Tween 80 appeared quite stable. Anise and Fennel EO-based formulations produced with Span 80 had a foamy consistency which made the sonication process impossible, therefore these two emulsions were discarded from subsequent analyses. In the non-sonicated emulsions, the droplets sizes were often within the micrometric range and presented high PDI values (0.25-1).

Among the sonicated formulations the smallest particle size was obtained using Tween 80 as surfactant ($H_{3,74}$=52.11; P<0.01), followed in order by Tween 20, Span 20 and Span 80. In terms of PDI values, Tween 80 and Tween 20 generated lower PDI values than the other two surfactants ($H_{3,74}$=45.56; P<0.01). Similar results were obtained considering the surface charge (ζ-potential); the nano-formulations containing Tween 80 and Tween 20 obtained ζ-potential values statistically different ($H_{3,74}$=50.62; P<0.01) from Span surfactants. Disregarding the different surfactants, the EOs used to develop the different sonicated formulations had a strong impact on particle size ($H_{6,71}$=24.07; P<0.01), ζ-potential ($H_{6,71}$=24.48; P<0.01), and PDI values ($H_{6,71}$=19.45; P<0.01).

The best combination in terms of particle size and PDI values were obtained when using Tween 80. This surfactant, coupled with sonication, contributed to produce particle size ranged from 116 ± 2 nm (Artemisia) to 188 ± 2 nm (Sage). Nevertheless, the PDI values (from 0.14 to 0.20) and the size were not correlated (ρ=0.364; P = 0.11); the lowest PDI value was recorded for the fennel EO-based formulation (0.14 ± 0.01), whereas the highest one was detected in the artemisia one (0.20±0.01). Among the sonicated nano-emulsions made with Tween 80, the employed EO affected all the physical parameters measured (Size: $H_{6,14}$=19.36; P<0.01 – PDI: $H_{6,14}$=12.66; P<0.05 – ζ-potential: $H_{6,14}$=18.92; P<0.01)

3.3 Evolution of nano-emulsion formulations over time

Tween 80 sonicated EO-based nano-emulsions were identified as the optimal formulations. Different physical parameters related to the Tween 80-based formulations were measured for 28 weeks from their production, to understand the evolution of the size, the PDI and the surface charge during storage. The developed nano-emulsions retained an average size of the droplets within the nanometre range either after 28 weeks of storage (**Figure 3**). Droplets sizes increased in all the evaluated formulations according to the storage duration ($H_{4,100}$=24.48; P<0.01) and it was affected by the EO used to develop the formulation ($H_{6,98}$=63.86; P<0.01). In sage and lavender EO-based formulations the

recorded droplet sizes increased from the fourth week of storage, exceeding the threshold of 250 nm, while the lowest increase of droplet dimension was reported for Artemisia EO-based nano-emulsion, whose average size was around 130 nm after 28 weeks of storage.

Furthermore, the low values of the PDI recorded just after a week from the emulsion preparation, indicated the size homogeneity of the formulations, since few or no aggregates were detected (**Figure 4**). Nevertheless, PDI values increased during storage in correlation with the size variations (ρ=0.859; P<0.01) and the time of storage ($H_{4,100}$=51.76; P<0.01). Artemisia nano-emulsion, which showed slight size changes during storage, also showed slight changes for PDI. In contrast, Sage formulation presented the highest PDI at 4 weeks, when the dimension of the droplets started to grow. Conversely, the PDI of anise and peppermint EO-based formulations remained quite stable until 14 weeks, but they presented a massive increase at 28 weeks, consistently with the increase of the droplet size.

All the EO nano-emulsion exhibited a negative ζ-potential, which ranged approximatively between -7 and -27 mV and the decline on the surface charge was time dependent ($H_{4,100}$=40.48; P<0.01) regardless of the EO used to formulate the nano-emulsions (**Figure 5**). Generally, ζ-potential remained stable for at least 2 weeks, when it started to decline. However, the decline of ζ-potential mainly depended on the EO oil employed for the formulation. The formulations made with fennel and rosemary EOs showed a great decrease after two weeks of storage, while other EO-based nano-emulsions, like anise and artemisia ones, had more constant patterns over time.

4. Discussion

In the current study, stable EO-based nano-emulsions with high relative amount of EO (i.e. 15%) were developed using a mixed bottom up/top down process (Sessa and Donsì, 2014). Nano-emulsions are perfect candidates for several applications, since they display characteristic qualities, as their ability to dissolve non-polar active compounds in water (Gutiérrez et al., 2008). The nano-dimensions generally improve both the stability and effectiveness of botanical extracts and active ingredients, boosting their gradual release (de Oliveira et al., 2014). However, the typical unstable nature of plant-based formulations is the key criticism to make these materials applicable for scale applications.

Generally, the self-emulsifying process, alone, did not produce nano-emulsions with small droplet size (Lombardo et al. 2020). In the current study, only few formulations (i.e. some EOs formulated with Tween 80) presented droplets with dimension ranging within the nanometric scale. It is known that the oil:surfactant ratio and the relative amount of the EO in the emulsion play a fundamental role in producing small droplet size and generally in improving the stability of EO-based nano-emulsions (Jesser

et al. 2020). In our study we used 3:1 oil:surfactant ratio and 15% of EO in all the nano-emulsions. The minimum droplet size in the non-sonicated nano-emulsion was about 180 nm for the formulation containing lavender EO and Tween 80, whereas, in most of the other EO/surfactant combinations, the droplet size was in the micrometric range. Several studies highlighted that the droplet size of nano-emulsions decreases with the decrease of the oil:surfactant ratio (Gulotta et al., 2014; Li et al., 2017; Saberi et al., 2013; Wang et al., 2009); thus, formulations containing high amount of surfactant could guarantee small droplets' dimension. In the current study, the different surfactants had an appreciable impact on both the droplet size and the PDI values. Among the tested surfactants, Tween 80 was able to produce the smallest droplets when compared with the other tested surfactants (Tween 20 Span 20 and Span 80). Similar results were reported by Chang et al. (2013), who obtained the smallest droplets in carvacrol-based nano-emulsions made with a mix of food-grade non-ionic surfactants (Tween 20, 40, 60, 80, and 85). Tweens, a class of non-ionic surfactants derived from sorbitan esters, are soluble or dispersible in water and are oil-in-water emulsifiers frequently used in pharmaceuticals, cosmetics and cleaning industries. Among these surfactants, Tween 80 is one of the most commonly used to develop EO-based insecticides. EO/surfactant combination is fundamental to attain valuable formulations. As example, two of the seven tested EOs (i.e. fennel and anise), when combined with Span 80, generated a dense foam impossible to sonicate. These two oils were characterized by the presence of (*E*)-anethole as their main constituent, whereas this molecule was absent or present only in small quantities in the other EOs; thus, (*E*)-anethole could be responsible for the formation of foam in presence of Span 80. In literature, (*E*)-anethole or anise-based nano-emulsions were usually produced using Tween 80 alone or in combination with co-surfactants (i.e. ethanol) (Hashem et al., 2018; Pascual-Villalobos et al., 2017).

Furthermore, the sonication process had a strong positive impact on both the droplet size and the PDI. This method is widely used for fabrication of nano-emulsions. The formation of fine droplets is due to the cavitation phenomenon that induces rapid changes, from vapor bubble formation to vapor bubble collapse, in liquids (Donsì and Ferrari, 2016). In the current study, the comparative study of various surfactants and emulsification processes highlighted that the sonicated nano-emulsions produced with Tween 80 had the best physical characteristics. The developed EO/Tween 80-based nano-emulsions presented small droplet size and good stability over time. Nevertheless, both size and stability seemed mainly dependent on the plant-source, since every EO-based formulation showed a peculiar size trend over time. The best results were obtained with artemisia EO, whose nano-emulsion was characterized by a size of 116 ± 2 nm and remained almost stable after 28 weeks of storage, with a droplet dimension of 128 ± 1 nm. In contrast, results for sage EO-based nano-emulsion presented the highest droplet size both at 1 week (188 ± 2 nm) and 28 weeks (260 ± 1) of storage. The difference of

droplet size and droplet stability can be related to the chemical composition of EOs. The molecular weight, polarity and conformation of volatile compounds as well as the presence of surface-active substances in EO can affect their water solubility and their capacity to form droplets with Tween. Artemisia EO is mainly constituted of oxygenated monoterpenes (82.52%) while composition of sage EO is more structurally diversified with monoterpenes (33.45%), oxygenated monoterpenes (56.19%) and sesquiterpene (7.68%). Surprisingly, main compounds of these two EOs are α-thujone (27.13% and 16.18%), β-thujone (13.25% and 4.42%), and camphor (21.45% and 12.64%) for artemisia and sage EOs, respectively. Lavender EO also contain camphor (6.88%) and high percentage of oxygenated monoterpenes (89.97%), but only artemisia based nano-emulsion is stable over 28 days. Finally, artemisia EO is characterized by the lowest content in sesquiterpenes (0.61%) while percentage of sesquiterpene is always over 2% in other EOs. It turns out that the most unstable nano-emulsions made from sage and lavender EOs are characterised by the highest content in sesquiterpene (7.68% and 4.33%, respectively). Even if it seems difficult to correlate droplet size stability to one or mix of compounds in this study, interesting results obtained with artemisia EO could be explain by a high percentage of oxygenated monoterpenes (i.e. α-thujone, β-thujone and camphor) combined with a low content in sesquiterpene. The good stability of the developed formulations was additionally supported by the low values of PDI recorded during the first storage phases (0.13-0.20). This characteristic seemed strongly linked to size increase, and PDI values tended to grow with increase in storage time. These results suggested that these nano-emulsions are not permanently stable, but a good stability of their characteristics may be guaranteed for long storage periods. The droplet dimensions obtained in the present study are consistent with previous studies on EO-based nano-emulsions containing lower oil:surfactant ratio (Hashem et al., 2018; Moghimi et al., 2016; Werdin González et al., 2014). As example, geranium EO-emulsions containing oil:surfactant (i.e. Tween 80) ratios of 1:05 to 1:1 showed dispersed phase diameters of 79 to 106 nm with high PDI values (around 0.3), that make them not stable after just three days (Jesser et al. 2020). In contrast, the nano-emulsions developed in the current study presented low PDI values, although the higher oil:surfactant ratio (3:1) used.

The developed nano-emulsion owed their stability mainly to steric-repulsion, considering that Tween 80 is a non-ionic surfactant. For this kind of emulsifier, osmotic forces can be substantial at distances of close interfacial approach, and they generally present greater order of magnitude than double layer repulsion and Van der Waals forces (Babchin and Schramm, 2012). Thus, artemisia formulation, which was noted as the most stable nano-emulsion presented the higher values of ζ-potential (from -10.6 to -7.6

mV). Nevertheless, the presence of a negative surface charges, which depends on the composition of oil, the pH and the electrolytes present in the water phase, may help to stabilize the nano-emulsions (Müller et al., 2001; Tadros et al., 2004). A minimum of ±30 mV of ζ-potential is required for a physically stable nano-suspension solely stabilized by electrostatic repulsion (Müller et al., 2001). The developed nano-emulsions in the present experimentation showed negative surface charge, which slightly increased during storage. To best of our knowledge, EO-based nano-emulsions prepared with non-ionic surfactant generally present negative surface charge (Acedo-Carrillo et al., 2006; Fernandes et al., 2014; Giunti et al., 2019; Hashem et al., 2018; Salvia-Trujillo et al., 2015). It has been acknowledged that this kind of surfactant can slightly alter the charge of the dispersed phase, depending on the covering surface created by the non-ionic surfactants (Li et al., 2016; Martins et al., 2012; Zhao et al., 2010). Hsu and Nacu (2003) demonstrated that an increasing concentration of non-ionic surfactant leads to ζ potential of the nano-emulsion nearest to zero, due to the highest coverage of the droplet surface by the non-charged surfactant molecules. According to several studies, the negative surface charge of EO-based nano-emulsions could be attributed to the dissociation of ionizable compound of the oils, which can be adsorbed on the droplet surface by the surfactant (Bonilla et al., 2012; Ge and Ge, 2016; Stachurski and Michalek, 1996). Furthermore, the absorption of negative ions (-OH) in the oil-water interface can change depending on the affinity between surfactant and oil, generating different ζ-potentials for different surfactant (Salvia-Trujillo et al., 2015). Hence, it is not surprising that, similar to size trends, ζ-potentials behaved differently on the basis of the plant species. Therefore, anise formulation had quite stable surface charge (between -20.57 and -17.4 mV), while fennel and rosemary displayed fluctuating ζ-potential (from about -26 to -12 mV).

The developed EO-based nano-formulations proposed in this paper showed good physical characteristics and excellent stability over time, making them suitable for industrial applications. To the best of our knowledge, this is the first time that EO-based nano-emulsion characteristics were reported during a medium-long storage period. The stability of formulations over time is a key issue for consideration in these EO-based nano-emulsions as biopesticides. This research highlighted the potential application of this methodology to pest control although further studies are required to evaluate the use of EO-based nano-emulsions under field conditions.

Funding

This research was supported by the project “Sustainable Tomato Production (STomP),” funded through the ARIMNet2 2015 Call by MIPAAF (Italy), ANR (France), DEMETER (Greece), MESRSFC (Morocco), and MHERS (Tunisia). ARIMNet2 (ERA-NET) has received funding from the European Union’s Seventh Framework Programme for research, technological development, and demonstration under grant agreement no. 618127.

CRediT authorship contribution statement

Orlando Campolo: Conceptualization, validation, writing, data analysis. **Giulia Giunti:** Metodology, formal analysis, validation, writing. **Vincenzo Palmeri:** Conceptualization, project administration, funding acquisition, writing. **Thomas Michel:** Conceptualization, writing, project administration, funding acquisition. **Maryne Laigle:** Metodology, formal analysis, validation, writing.

5. References

Acedo-Carrillo, J.I., Rosas-Durazo, A., Herrera-Urbina, R., Rinaudo, M., Goycoolea, F.M., Valdez, M.A., 2006. Zeta potential and drop growth of oil in water emulsions stabilized with mesquite gum. Carbohydr. Polym. 65, 327–336. https://doi.org/10.1016/j.carbpol.2006.01.016

Anarjan, N., Jaberi, N., Yeganeh-Zare, S., Banafshehchin, E., Rahimirad, A., Jafarizadeh-Malmiri, H., 2014. Optimization of mixing parameters for α-tocopherol nanodispersions prepared using solvent displacement method. J. Am. Oil Chem. Soc. 91, 1397-1405. https://doi.org/10.1007/s11746-014-2482-6

Asbahani, A. El, Miladi, K., Badri, W., Sala, M., Addi, E.H.A., Casabianca, H., Mousadik, A. El, Hartmann, D., Jilale, A., Renaud, F.N.R., Elaissari, A., 2015. Essential oils: From extraction to encapsulation. Int. J. Pharm. 483, 220–243. https://doi.org/10.1016/J.IJPHARM.2014.12.069

Babchin, A.J., Schramm, L.L., 2012. Osmotic repulsion force due to adsorbed surfactants. Colloids Surfaces B Biointerfaces 91, 137–143. https://doi.org/10.1016/j.colsurfb.2011.10.050

Bakkali, F., Averbeck, S., Averbeck, D., Idaomar, M., 2008. Biological effects of essential oils – A review. Food Chem. Toxicol. 46, 446–475.

Baskar, K., Sudha, V., Nattudurai, G., Ignacimuthu, S., Duraipandiyan, V., Jayakumar, M., Al-Dhabi, N.A., Benelli, G., 2018. Larvicidal and repellent activity of the essential oil from Atalantia monophylla on three mosquito vectors of public health importance, with limited impact on non-target zebra fish. Physiol. Mol. Plant Pathol. 101, 197–201. https://doi.org/10.1016/j.pmpp.2017.03.002

Benelli, G., 2015. Plant-borne ovicides in the fight against mosquito vectors of medical and veterinary importance: a systematic review. Parasitol. Res. 114, 3201–12. https://doi.org/10.1007/s00436-015-4656-z

Bonilla, J., Atarés, L., Vargas, M., Chiralt, A., 2012. Effect of essential oils and homogenization conditions on properties of chitosan-based films. Food Hydrocoll. 26, 9–16. https://doi.org/10.1016/j.foodhyd.2011.03.015

Bouchemal, K., Briançon, S., Perrier, E., Fessi, H., 2004. Nano-emulsion formulation using spontaneous emulsification: solvent, oil and surfactant optimisation. Int. J. Pharm. 280, 241–251. https://doi.org/10.1016/J.IJPHARM.2004.05.016

Burger, P., Plainfossé, H., Brochet, X., Chemat, F., Fernandez, X., 2019. Extraction of Natural Fragrance Ingredients: History Overview and Future Trends. Chem. Biodivers.

16. https://doi.org/10.1002/cbdv.201900424

Campolo, O., Cherif, A., Ricupero, M., Siscaro, G., Grissa-Lebdi, K., Russo, A., Cucci, L.M., Di Pietro, P., Satriano, C., Desneux, N., Biondi, A., Zappalà, L., Palmeri, V., 2017. Citrus peel essential oil nanoformulations to control the tomato borer, Tuta absoluta: chemical properties and biological activity. Sci. Rep. 7, 13036. https://doi.org/10.1038/s41598-017-13413-0

Campolo, O., Giunti, G., Russo, A., Palmeri, V., Zappalà, L., 2018. Essential Oils in Stored Product Insect Pest Control. J. Food Qual. 2018, 1–18. https://doi.org/10.1155/2018/6906105

Chang, Y., McLandsborough, L., McClements, D.J., 2013. Physicochemical properties and antimicrobial efficacy of carvacrol nanoemulsions formed by spontaneous emulsification. J. Agric. Food Chem. 61, 8906–8913. https://doi.org/10.1021/jf402147p

De Almeida, L.F.R., Frei, F., Mancini, E., De Martino, L., De Feo, V., 2010. Phytotoxic activities of Mediterranean essential oils. Molecules 15, 4309–4323. https://doi.org/10.3390/molecules15064309

de Oliveira, J.L., Campos, E.V.R., Bakshi, M., Abhilash, P.C., Fraceto, L.F., 2014. Application of nanotechnology for the encapsulation of botanical insecticides for sustainable agriculture: Prospects and promises. Biotechnol. Adv. 32, 1550–1561. https://doi.org/10.1016/J.BIOTECHADV.2014.10.010

Do, T.K.T., Hadji-Minaglou, F., Antoniotti, S., Fernandez, X., 2015. Authenticity of essential oils. TrAC - Trends Anal. Chem. https://doi.org/10.1016/j.trac.2014.10.007

Donsì, F., Ferrari, G., 2016. Essential oil nanoemulsions as antimicrobial agents in food. J. Biotechnol. https://doi.org/10.1016/j.jbiotec.2016.07.005

Fernandes, C., de Almeida, F., Silveira, A., Gonzalez, M., Mello, C., Feder, D., Apolinário, R., Santos, M., Carvalho, J.C., Tietbohl, L.A., Rocha, L., Falcão, D., 2014. Development of an insecticidal nanoemulsion with Manilkara subsericea (Sapotaceae) extract. J. Nanobiotechnology 12, 22. https://doi.org/10.1186/1477-3155-12-22

Ge, Y., Ge, M., 2016. Distribution of *Melaleuca alternifolia* essential oil in liposomes with Tween 80 addition and enhancement of *in vitro* antimicrobial effect. J. Exp. Nanosci. 11, 345–358. https://doi.org/10.1080/17458080.2015.1065013

Giunti, G., Palermo, D., Laudani, F., Algeri, G.M., Campolo, O., Palmeri, V., 2019. Repellence and acute toxicity of a nano-emulsion of sweet orange essential oil toward two major stored grain insect pests. Ind. Crops Prod. 142, 111869. https://doi.org/10.1016/j.indcrop.2019.111869

Gulotta, A., Saberi, A.H., Nicoli, M.C., McClements, D.J., 2014. Nanoemulsion-based delivery systems for polyunsaturated (ω-3) oils: Formation using a spontaneous emulsification method. J. Agric. Food Chem. 62, 1720–1725. https://doi.org/10.1021/jf4054808

Gutiérrez, J.M., González, C., Maestro, A., Solè, I., Pey, C.M., Nolla, J., 2008. Nano-emulsions: New applications and optimization of their preparation. Curr. Opin. Colloid Interface Sci. 13, 245–251. https://doi.org/10.1016/J.COCIS.2008.01.005

Hashem, A.S., Awadalla, S.S., Zayed, G.M., Maggi, F., Benelli, G., 2018. Pimpinella anisum essential oil nanoemulsions against Tribolium castaneum-insecticidal activity and mode of action. Environ. Sci. Pollut. Res. 25, 18802–12. https://doi.org/10.1007/s11356-018-2068-1

He, X., Deng, H., Hwang, H. min, 2019. The current application of nanotechnology in food and agriculture. J. Food Drug Anal. https://doi.org/10.1016/j.jfda.2018.12.002

Hess, F.D., Foy, C.L., 2000. Interaction of Surfactants with Plant Cuticles. Weed Technol. 14, 807–813. https://doi.org/10.1614/0890-037x(2000)014[0807:ioswpc]2.0.co;2

Hsu, J.P., Nacu, A., 2003. Behavior of soybean oil-in-water emulsion stabilized by nonionic surfactant. J. Colloid Interface Sci. 259, 374–381. https://doi.org/10.1016/S0021-9797(02)00207-2

Hurtt, W., Hodgson, R.H., 1987. Effects of Nonionic Surfactants, Temperature, and Light on Germination of Weed Seeds. Weed Sci. 35, 52–57. https://doi.org/10.1017/s0043174500026771

Ibáñez, M.D., Blázquez, M.A., 2020. Phytotoxic effects of commercial essential oils on selected vegetable crops: Cucumber and tomato. Sustain. Chem. Pharm. 15, 100209. https://doi.org/10.1016/j.scp.2019.100209

Isman, M.B., Grieneisen, M.L., 2014. Botanical insecticide research: Many publications, limited useful data. Trends Plant Sci. https://doi.org/10.1016/j.tplants.2013.11.005

Isman, M.B., Seffrin, R., Seffrin, R., 2018. Essential Oils as Green Pesticides for Plant Protection in Horticulture 217–260. https://doi.org/10.1201/B2243

Jesser, E., Lorenzetti, A. S., Yeguerman, C., Murray, A. P., Domini, C., Werdin-González, J. O., 2020. Ultrasound assisted formation of essential oil nanoemulsions: Emerging alternative for *Culex pipiens pipiens* Say (Diptera: Culicidae) and *Plodia interpunctella* Hübner (Lepidoptera: Pyralidae) management. Ultrason. Sonochem. 61, 104832. https://doi.org/10.1016/j.ultsonch.2019.104832

Karalija, E., Dahija, S., Parić, A., Ćavar Zeljković, S., 2020. Phytotoxic potential of selected essential oils against Ailanthus altissima (Mill.) Swingle, an invasive tree.

Sustain. Chem. Pharm. 15, 100219. https://doi.org/10.1016/j.scp.2020.100219

Li, J., Chang, J.W., Saenger, M., Deering, A., 2017. Thymol nanoemulsions formed via spontaneous emulsification: Physical and antimicrobial properties. Food Chem. 232, 191–197. https://doi.org/10.1016/j.foodchem.2017.03.147

Li, X., Qin, Y., Liu, C., Jiang, S., Xiong, L., Sun, Q., 2016. Size-controlled starch nanoparticles prepared by self-assembly with different green surfactant: The effect of electrostatic repulsion or steric hindrance. Food Chem. 199, 356–363. https://doi.org/10.1016/j.foodchem.2015.12.037

Liu, Z., 2004. Effects of surfactants on foliar uptake of herbicides - A complex scenario. Colloids Surfaces B Biointerfaces 35, 149–153. https://doi.org/10.1016/j.colsurfb.2004.02.016

Lombardo, D., Calandra, P., Pasqua, L., Magazù, S., 2020. Self-Assembly of Organic Nanomaterials and Biomaterials: The Bottom-Up Approach for Functional Nanostructures Formation and Advanced Applications. Materials 13, 1048. https://doi.org/10.3390/ma13051048

Martins, S., Tho, I., Souto, E., Ferreira, D., Brandl, M., 2012. Multivariate design for the evaluation of lipid and surfactant composition effect for optimisation of lipid nanoparticles. Eur. J. Pharm. Sci. 45, 613–623. https://doi.org/10.1016/j.ejps.2011.12.015

Mirgorodskaya, A.B., Kushnazarova, R., Lukashenko, S.S., Nikitin, E.N., Sinyashin, K.O., Nesterova, L.M., Zakharova, L.Y., 2020. Carbamate-bearing surfactants as effective adjuvants promoted the penetration of the herbicide into the plant. Colloids Surfaces A Physicochem. Eng. Asp. 586, 124252. https://doi.org/10.1016/j.colsurfa.2019.124252

Moghimi, R., Ghaderi, L., Rafati, H., Aliahmadi, A., McClements, D.J., 2016. Superior antibacterial activity of nanoemulsion of Thymus daenensis essential oil against E. coli. Food Chem. 194, 410–415. https://doi.org/10.1016/J.FOODCHEM.2015.07.139

Müller, R.., Jacobs, C., Kayser, O., 2001. Nanosuspensions as particulate drug formulations in therapy: Rationale for development and what we can expect for the future. Adv. Drug Deliv. Rev. 47, 3–19. https://doi.org/10.1016/S0169-409X(00)00118-6

Niedobová, J., Skalský, M., Ouředníčková, J., Michalko, R., Bartošková, A., 2019. Synergistic effects of glyphosate formulation herbicide and tank-mixing adjuvants on Pardosa spiders. Environ. Pollut. 249, 338–344. https://doi.org/10.1016/j.envpol.2019.03.031

O'Donovan, J.T., O'Sullivan, P.A., Caldwell, C.D., 1985. Basis for changes in glyphosate phytotoxicity to barley by the non-ionic surfactants Tween 20 and Renex 36*. Weed Res. 25, 81–86. https://doi.org/10.1111/j.1365-3180.1985.tb00621.x

Pascual-Villalobos, M.J., Cantó-Tejero, M., Vallejo, R., Guirao, P., Rodríguez-Rojo, S., Cocero, M.J., 2017. Use of nanoemulsions of plant essential oils as aphid repellents. Ind. Crops Prod. 110, 45–57. https://doi.org/10.1016/j.indcrop.2017.05.019

Pavela, R., 2015. Essential oils for the development of eco-friendly mosquito larvicides: A review. Ind. Crops Prod. 76, 174–187. https://doi.org/10.1016/j.indcrop.2015.06.050

Pavela, R., Benelli, G., 2016. Essential Oils as Ecofriendly Biopesticides? Challenges and Constraints. Trends Plant Sci. 21, 1000–1007. https://doi.org/10.1016/J.TPLANTS.2016.10.005

Regnault-Roger, C., Vincent, C., Arnason, J.T., 2012. Essential Oils in Insect Control: Low-Risk Products in a High-Stakes World. Annu. Rev. Entomol. 57, 405–424. https://doi.org/10.1146/annurev-ento-120710-100554

Rodríguez, J., Martín, M.J., Ruiz, M.A., Clares, B., 2016. Current encapsulation strategies for bioactive oils: From alimentary to pharmaceutical perspectives. Food Res. Int. https://doi.org/10.1016/j.foodres.2016.01.032

Saberi, A.H., Fang, Y., McClements, D.J., 2013. Fabrication of vitamin E-enriched nanoemulsions: Factors affecting particle size using spontaneous emulsification. J. Colloid Interface Sci. 391, 95–102. https://doi.org/10.1016/j.jcis.2012.08.069

Salvia-Trujillo, L., Rojas-Graü, A., Soliva-Fortuny, R., Martín-Belloso, O., 2015. Physicochemical characterization and antimicrobial activity of food-grade emulsions and nanoemulsions incorporating essential oils. Food Hydrocoll. 43, 547–556. https://doi.org/10.1016/j.foodhyd.2014.07.012

Sessa, M., Donsì, F. (2015). Nanoemulsion-based delivery systems. In Microencapsulation and microspheres for food applications (pp. 79-94). Academic Press, Cambridge, USA

Stachurski, J., Michalek, M., 1996. The effect of the ζ potential on the stability of a non-polar oil-in-water emulsion. J. Colloid Interface Sci. 184, 433–436. https://doi.org/10.1006/jcis.1996.0637

Svoboda, K.., Greenaway, R.., 2003. Investigation of volatile oil glands of Satureja hortensis L. (summer savory) and phytochemical comparison of different varieties. Int. J. Aromather. 13, 196–202. https://doi.org/10.1016/S0962-4562(03)00038-9

Tadros, T., Izquierdo, P., Esquena, J., Solans, C., 2004. Formation and stability of nano-emulsions. Adv. Colloid Interface Sci. 108–109, 303–318. https://doi.org/10.1016/J.CIS.2003.10.023

Wang, L., Dong, J., Chen, J., Eastoe, J., Li, X., 2009. Design and optimization of a new self-nanoemulsifying drug delivery system. J. Colloid Interface Sci. 330, 443–448. https://doi.org/10.1016/j.jcis.2008.10.077

Werdin González, J.O., Gutiérrez, M.M., Ferrero, A.A., Fernández Band, B., 2014. Essential oils nanoformulations for stored-product pest control – Characterization and biological properties. Chemosphere 100, 130–138. https://doi.org/10.1016/J.CHEMOSPHERE.2013.11.056

Zhao, Y., Wang, C., Chow, A.H.L., Ren, K., Gong, T., Zhang, Z., Zheng, Y., 2010. Self-nanoemulsifying drug delivery system (SNEDDS) for oral delivery of Zedoary essential oil: Formulation and bioavailability studies. Int. J. Pharm. 383, 170–177. https://doi.org/10.1016/j.ijpharm.2009.08.035

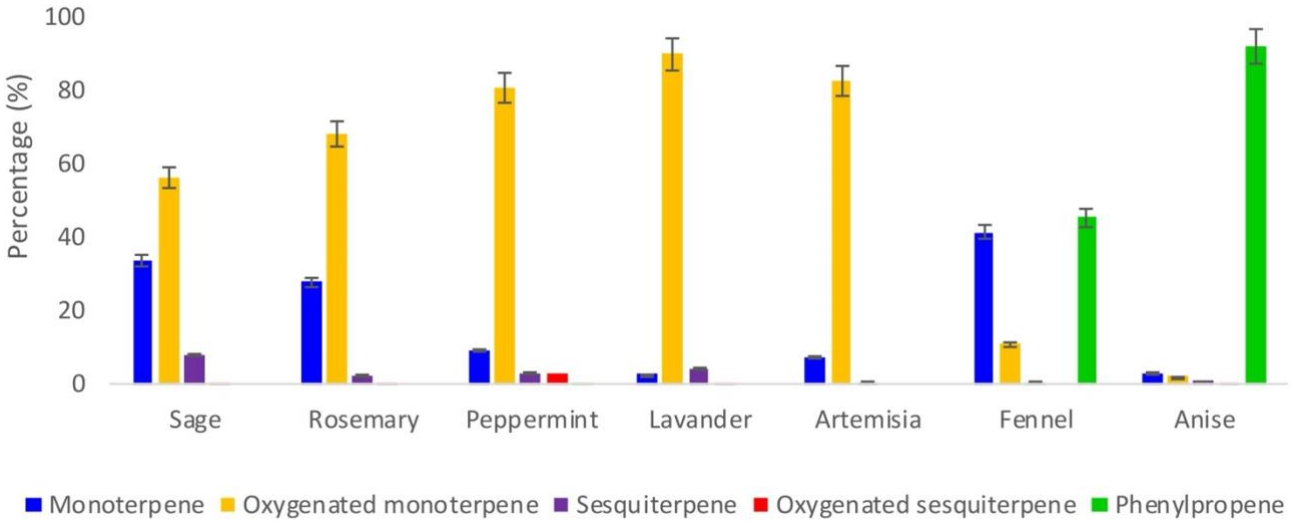

Figure 1: Percentage of main classes of volatile compounds characterized in the essential oils of different species.

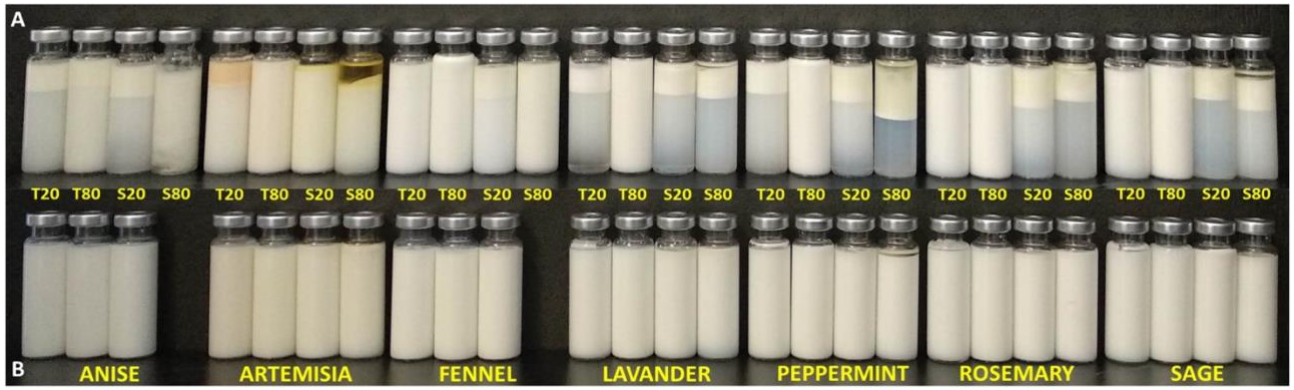

Figure 2: Essential oil-based nano-emulsions. A) Before sonication (24h from preparation); B) After sonication (24h from sonication). Surfactant: T20= Tween 20; T80= Tween 80; S20=Span 20; S80=Span 80. Some not sonicated formulations (Anise-S80 and Fennel-S80) were not suitable for the sonication process.

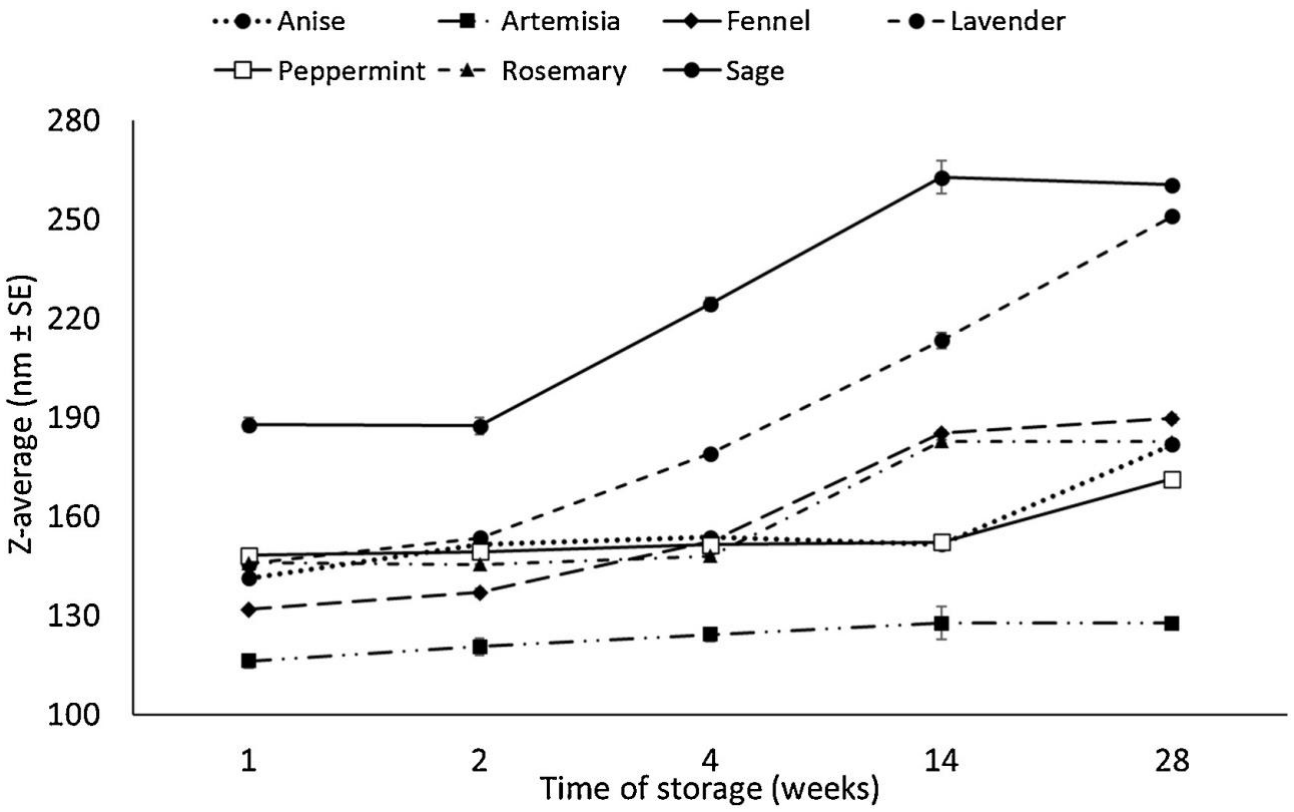

Figure 3 Mean Z-average (± SE) of Tween 80 sonicated EO-based nano-emulsions over 28 weeks of storage (n=3). Values are means of triplicates. Vertical bars indicate standard errors.

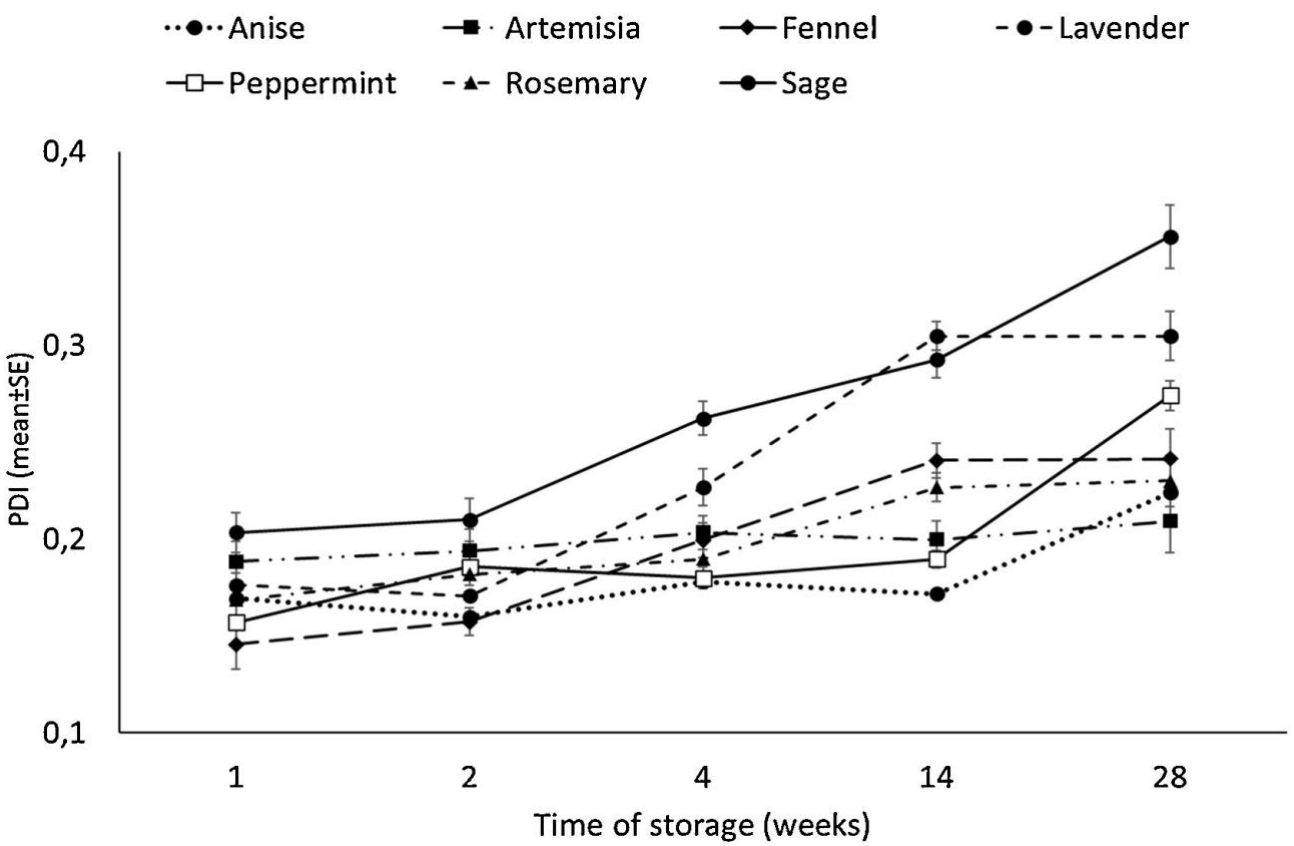

Figure 4 Mean PolyDispersion Index (± SE) of Tween 80 sonicated EO-based nano-emulsions over 28 weeks of storage (n=3). Values are means of triplicates. Vertical bars indicate standard errors.

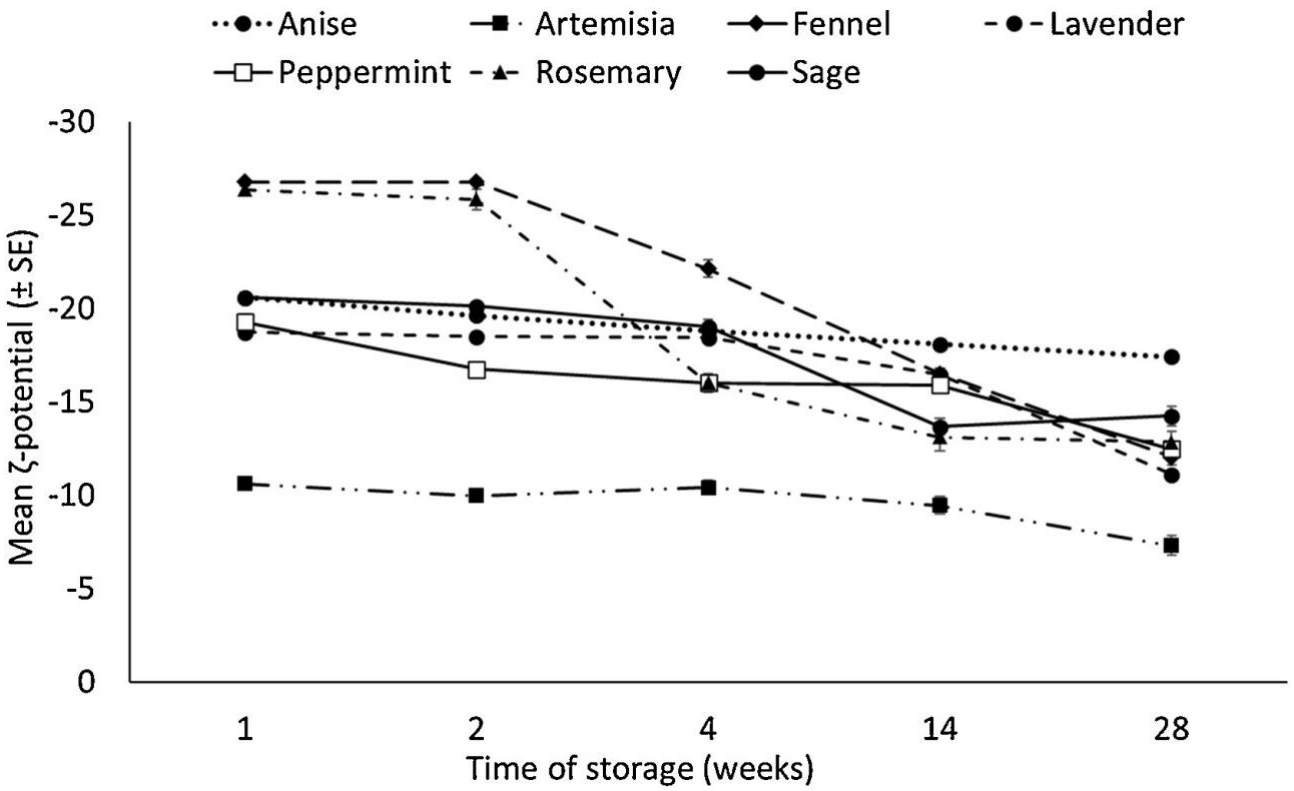

Figure 5 Mean ζ-potential (± SE) of Tween 80 sonicated EO-based nano-emulsions over 28 weeks of storage (n=3). Values are means of triplicates. Vertical bars indicate standard errors.

Supplementary material

Table S1: Chemical composition of sage essential oil (n=3).

Class	Constituents	RI calc. HP-1	RI litt. HP-1	%± SD
Monoterpene	tricyclene	924	920	0.39 ± 0.0
Monoterpene	α-thujene	928	924	0.21 ± 0.0
Monoterpene	α-pinene	934	932	19.18 ± 0.002
Monoterpene	camphene	947	946	4.44 ± 0.0
Monoterpene	β-pinene	974	972	3.67 ± 0.0
Monoterpene	myrcene	989	983	0.90 ± 0.0
Monoterpene	α-phellandrene	1002	997	0.09 ± 0.0
Monoterpene	α-terpinene	1014	1009	0.67 ± 0.0
Monoterpene	para-cymene	1018	1014	2.23 ± 0.0
Oxygenated monoterpene	eucalyptol	1026	1022	19.08 ± 0.001
Monoterpene	γ-terpinene	1054	1051	1.26 ± 0.0
Monoterpene	terpinolene	1085	1080	0.41 ± 0.0
Oxygenated monoterpene	α-thujone	1093	1097	16.18 ± 0.002
Oxygenated monoterpene	β-thujone	1103	1110	4.42 ± 0.0
Oxygenated monoterpene	camphor	1129	1123	12.64 ± 0.001
Oxygenated monoterpene	borneol	1161	1154	2.59 ± 0.0
Oxygenated monoterpene	(-)-bornyl acetate	1279	1273	1.11 ± 0.0
Oxygenated monoterpene	thymol	1292	1277	0.17 ± 0.0
Sesquiterpene	longifolene	1412	1398.3	0.42 ± 0.0
Sesquiterpene	β-caryophyllene	1425	1420	3.49 ± 0.0
Sesquiterpene	α-humulene	1459	1449	3.73 ± 0.0
Oxygenated sesquiterpene	caryophyllene oxyde	1582	1568	0.10 ± 0.0
Sesquiterpene	δ-guaiene	1485	1485	0.04 ± 0.0
Monoterpene				**33.45 ± 0.1**
Oxygenated monoterpene				**56.19 ± 0.2**
Sesquiterpene				**7.68 ± 0.001**
Oxygenated sesquiterpene				**0.10 ± 0.0**
Total				**97.42 ± 0.3**

0

Table S2: Chemical composition of rosemary essential oil (n=3).

Class	Constituents	RI calc. HP-1	RI litt. HP-1	% ± SD
Monoterpene	α-pinene	934	932	11.78 ± 0.001
Monoterpene	camphene	947	946	2.82 ± 0.0
Monoterpene	Sabinene	971	968	0.17 ± 0.0
Monoterpene	β-pinene	974	972	4.06 ± 0.0
Monoterpene	myrcene	989	983	1.10 ± 0.0
Monoterpene	α-phellandrene	1001	993	0.34 ± 0.0
Monoterpene	δ-3-carene	1010	1006	0.35 ± 0.0
Monoterpene	α-terpinene	1013	1009	1.79 ± 0.0
Monoterpene	ortho-cymene	1019	1019	4.18 ± 0.0
Oxygenated monoterpene	eucalyptol	1027	1022	52.58 ± 0.1
Monoterpene	cis-β-ocimene	1033	1024	0.07 ± 0.0
Monoterpene	γ-terpinene	1055	1051	0.84 ± 0.0
Monoterpene	terpinolene	1085	1080	0.18 ± 0.0
Oxygenated monoterpene	linalol	1095	1086	0.43 ± 0.0
Oxygenated monoterpene	camphor	1129	1123	11.84 ± 0.001
Oxygenated monoterpene	Unknown 1	1135	/	0.07 ± 0.0
Oxygenated monoterpene	Unknown 2	1158	/	0.18 ± 0.0
Oxygenated monoterpene	borneol	1161	1154	1.45 ± 0.0
Oxygenated monoterpene	terpinen-4-ol	1171	1165	0.42 ± 0.0
Oxygenated monoterpene	α-terpineol	1183	1175	0.93 ± 0.0
Oxygenated monoterpene	bornyl acetate	1279	1273	0.44 ± 0.0
Sesquiterpene	α-ylangene	1377	1370	0.04 ± 0.0
Sesquiterpene	α-copaene	1381	1374	0.14 ± 0.0
Sesquiterpene	longifolene	1410	1398	0.11 ± 0.0
Sesquiterpene	β-caryophyllene	1425	1420	1.90 ± 0.0
Sesquiterpene	β-cadinene	1515	1511	0.01 ± 0.0
Sesquiterpene	δ-cadinene	1524	1516	0.20 ± 0.0
Oxygenated sesquiterpene	caryophyllene oxyde	1581	1568	0.11 ± 0.0
Monoterpene				**27.68 ± 0.01**
Oxygenated monoterpene				**68.34 ± 0.15**
Sesquiterpene				**2.4 ± 0.0**
Oxygenated sesquiterpene				**0.11 ± 0.0**
Total				**98. 53 ± 0.15**

Table S3: Chemical composition of peppermint essential oil (n=3).

Class	Constituents	RI calc. HP-1	RI litt. HP-1	% ± SD
Monoterpene	α-pinene	934	932	1.03 ± 0.0
Monoterpene	sabinene	971	968	0.39 ± 0.0
Monoterpene	β-pinene	974	972	1.24 ± 0.0
Monoterpene	myrcene	989	983	0.50 ± 0.0
Monoterpene	limonene	1026	1025	6.11 ± 0.0
Oxygenated monoterpene	eucalyptol	1026	1022	3.59 ± 0.0
Oxygenated monoterpene	menthone	1140	1141	18.47 ± 0.01
Oxygenated monoterpene	isomenthone	1149	1147	6.78 ± 0.0
Oxygenated monoterpene	menthofurane	1156	1150	1.02 ± 0.0
Oxygenated monoterpene	(-) neomenthol	1159	1157	4.89 ± 0.0
Oxygenated monoterpene	(-) menthol	1170	1167	38.63 ± 0.05
Oxygenated monoterpene	α-terpineol	1184	1175	0.58 ± 0.0
Oxygenated monoterpene	pulegone	1224	1217	1.10 ± 0.0
Oxygenated monoterpene	S-(+)carvone	1226	1219	0.68 ± 0.0
Oxygenated monoterpene	piperitone	1237	1231	0.85 ± 0.0
Oxygenated monoterpene	isomenthyl acetate	1270	1289	0.15 ± 0.0
Phenylpropenes	(E)-anethole	1274	1269	2.97 ± 0.0
Oxygenated monoterpene	menthyl acetate	1286	1279	3.68 ± 0.0
Sesquiterpene	β-bourbonene	1389	1381	0.24 ± 0.0
Sesquiterpene	β-elemene	1395	1386	0.13 ± 0.0
Sesquiterpene	β-caryophyllene	1425	1420	1.25 ± 0.0
Sesquiterpene	β-cubebene	1433	1388	0.07 ± 0.0
Sesquiterpene	calarene	1457	1428	0.15 ± 0.0
Sesquiterpene	α-humulene	1459	1449	0.09 ± 0.0
Sesquiterpene	γ-muurolene	1479	1473	0.03 ± 0.0
Sesquiterpene	germacrene D	1484	1476	0.42 ± 0.0
Sesquiterpene	germacrene B	1501	1544	0.11 ± 0.0
Sesquiterpene	γ-cadinene	1515	1511	0.03 ± 0.0
Sesquiterpene	δ-cadinene	1524	1516	0.08 ± 0.0
Oxygenated sesquiterpene	(+) spathulenol	1579	1566	0.03 ± 0.0
Oxygenated sesquiterpene	caryophyllene oxyde	1582	1568	0.07 ± 0.0
Monoterpene				**9.27 ± 0.0**
Oxygenated monoterpene				**80.43 ± 0.1**
Sesquiterpene				**2.6 ± 0.0**
Oxygenated sesquiterpene				**0.1 ± 0.0**
Phenylpropenes				**2.97 ± 0.0**
Total				**95.37 ± 0.1**

Table S4: Chemical composition of lavender essential oil (n=3).

Class	Constituents	RI calc. HP-1	RI litt. HP-1	%± SD
Monoterpene	α-thujene	928	924	0.04 ± 0.0
Monoterpene	α-pinene	934	932	0.57 ± 0.0
Monoterpene	camphene	948	945	0.14 ± 0.0
Monoterpene	sabinene	971	968	0.14 ± 0.0
Monoterpene	β-pinene	975	972	0.20 ± 0.0
Monoterpene	myrcene	989	983	0.27 ± 0.0
Monoterpene	*p*-cymene	1018	1014	0.27 ± 0.0
Oxygenated monoterpene	eucalyptol	1026	1022	5.51 ± 0.0
Monoterpene	(Z)-β-ocimene	1033	1024	0.63 ± 0.0
Monoterpene	(E)-β-ocimene	1044	1037	0.31 ± 0.0
Oxygenated monoterpene	γ-terpinene	1055	1051	0.10 ± 0.0
Oxygenated monoterpene	trans-Sabinene hydrate	1063	1058	0.11 ± 0.0
Oxygenated monoterpene	linalol oxyde	1069	1062	0.06 ± 0.0
Monoterpene	terpinolene	1085	1080	0.07 ± 0.0
Oxygenated monoterpene	linalol	1097	1086	38.13 ± 0.1
Oxygenated monoterpene	camphor	1129	1123	6.68 ± 0.0
Oxygenated monoterpene	isoborneol	1153	1143	0.38 ± 0.0
Oxygenated monoterpene	borneol	1161	1154	2.25 ± 0.0
Oxygenated monoterpene	terpinen-4-ol	1171	1165	1.67 ± 0.0
Ester	hexyl butyrate	1181	1182	0.39 ± 0.0
Oxygenated monoterpene	α-terpineol	1183	1175	0.26± 0.0
Oxygenated monoterpene	linalyl acetate	1252	1243	33.42 ± 0.1
Oxygenated monoterpene	lavandulyl acetate	1282	1273	1.11 ± 0.0
Sesquiterpene	δ-elemene	1343	1337	0.03± 0.0
Oxygenated monoterpene	geranyl acetate	1371	1363	0.19 ± 0.0
Sesquiterpene	(-)-α-copaene	1381	1374	0.11 ± 0.0
Sesquiterpene	daucene	1386	1380	0.06 ± 0.0
Sesquiterpene	unknown 1	1407	/	0.05 ± 0.0
Sesquiterpene	α-cedrene	1418	1411	0.03 ± 0.0
Sesquiterpene	β-caryophyllene	1425	1420	2.16 ± 0.0
Sesquiterpene	unknown 2	1439	/	0.20 ± 0.0
Sesquiterpene	β-farnesene	1454	1457	0.58 ± 0.0
Sesquiterpene	α-humulene	1459	1449	0.24 ± 0.0
Sesquiterpene	α-elemene	1474	1493	0.05 ± 0.0
Sesquiterpene	γ-muurolene	1479	1473	0.06 ± 0.0
Sesquiterpene	germacrene D	1484	1476	0.36 ± 0.0
Sesquiterpene	α-bisabolene	1508	1504	0.13± 0.0
Sesquiterpene	γ-cadinene	1515	1511	0.14 ± 0.0
Sesquiterpene	β-sesquiphellandrene	1521	1524	0.13 ± 0.0
Oxygenated sesquiterpene	caryophyllene oxyde	1582	1568	0.10 ± 0.0
Oxygenated sesquiterpene	α-bisabolol	1678	1672	0.12 ± 0.0
Ester				**0.39 ± 0.0**
Monoterpene				**2.64 ± 0.0**

Oxygenated monoterpene	**89.87 ± 0.2**
Sesquiterpene	**4.33 ± 0.0**
Oxygenated sesquiterpene	**0.22 ± 0.0**
Total	**97.45 ± 0.2**

Table S5: Chemical composition of artemisia essential oil (n=3).

Class	Constituents	RI calc. HP-1	RI litt. HP-1	% ± SD
Monoterpene	unknonw 1	850.8	855	0.13 ± 0.0
Monoterpene	tricyclene	923.6	920	0.32 ± 0.0
Monoterpene	α-pinene	934.4	932	0.58 ± 0.0
Monoterpene	camphene	946.8	946	4.04 ± 0.0
Monoterpene	verbenene	952.9	950	0.15 ± 0.0
Monoterpene	sabinene	970.4	968	0.62 ± 0.0
Monoterpene	β-pinene	974.8	972	0.09 ± 0.0
Aromatic hydrocarbon	1,2,4-trimethylbenzene	986.0	986	0.20 ± 0.0
Monoterpene	myrcene	989.2	983	0.13 ± 0.0
Monoterpene	α-phellandrene	1001.8	997	0.08 ± 0.0
Aromatic hydrocarbon	1,2,3-trimethylbenzene	1013.9	1010	0.20 ± 0.0
Monoterpene	*p*-cymene	1017.8	1010	0.96 ± 0.0
Monoterpene	β-phellandrene	1024.9	1021	0.14± 0.0
Oxygenated monoterpene	eucalyptol	1026	1022	4.09 ± 0.0
Oxygenated monoterpene	γ-terpinene	1054.7	1051	0.29 ± 0.0
Oxygenated monoterpene	terpinolene	1085.3	1080	0.14 ± 0.0
Oxygenated monoterpene	nonanal	1089.0	1080	1.10 ± 0.0
Oxygenated monoterpene	α-thujone	1093.4	1088	27.13 ± 0.01
Oxygenated monoterpene	β-thujone	1104	1110	13.25 ± 0.001
Oxygenated monoterpene	chrysanthenone	1109.3	1102	6.12 ± 0.0
Oxygenated monoterpene	(Z)-β-terpineol	1118.2	1120	0.14 ± 0.0
Oxygenated monoterpene	camphor	1129.6	1123	21.45 ± 0.01
Oxygenated monoterpene	trans-pinocarveol	1134.6	1128	0.93 ± 0.0
Oxygenated monoterpene	pinocarvone	1148.7	1138	0.18 ± 0.0
Oxygenated monoterpene	borneol	1161.8	1154	0.66 ± 0.0
Oxygenated monoterpene	terpinene-4-ol	1170.7	1165	0.66 ± 0.0
Oxygenated monoterpene	chrysantenyl acetate	1255.7	1216	4.68 ± 0.0
Oxygenated monoterpene	isobornyl acetate	1279.5	1276	0.44 ± 0.0
Oxygenated monoterpene	sabinyl acetate	1283.4	1282	0.25 ± 0.0
Oxygenated monoterpene	eucarvone	1376.0	1327	1.01 ± 0.0
Sesquiterpene	alpha-copaene	1381.0	1374	0.18 ± 0.0
Sesquiterpene	germacrene D	1483.7	1476	0.37 ± 0.0
Sesquiterpene	germacrene B	1500.4	1544	0.06 ± 0.0
Aromatic hydrocarbon				**0.40 ± 0.0**
Monoterpene				**7.24 ± 0.0**
Oxygenated monoterpene				**82.52 ± 0.05**
Sesquiterpene				**0.61 ± 0.0**
Total				**90.77 ± 0.05**

Table S6: Chemical composition of fennel essential oil (n=3).

Class	Constituents	RI calc. HP-1	RI litt. HP-1	% ± SD
Monoterpene	α-pinene	934	936	2.33 ± 0.0
Monoterpene	camphene	948	946	0.28 ± 0.0
Monoterpene	sabinene	971	968	0.11 ± 0.0
Monoterpene	β-pinene	974	977	0.88 ± 0.0
Monoterpene	β-myrcene	989	983	1.04 ± 0.0
Monoterpene	α-phellandrene	1001	1003	2.68 ± 0.0
Monoterpene	δ-3-carene	1010	1006	0.28 ± 0.0
Monoterpene	α-terpinene	1014	1009	0.36 ± 0.0
Monoterpene	*p*-cymene	1018	1025	1.70 ± 0.0
Monoterpene	limonene	1027	1029	30.84 ± 0.01
Monoterpene	(Z)-β-ocimene	1033	1024	0.50 ± 0.0
Monoterpène	γ-terpinene	1055	1051	0.17 ± 0.0
Oxygenated monoterpene	fenchone	1075	1072	9.88 ± 0.0
Monoterpène	Terpinolene	1085	1080	0.20 ± 0.0
Oxygenated monoterpene	linalol	1094	1086	0.59 ± 0.0
Oxygenated monoterpene	camphor	1129	1123	0.1± 0.0 4
Oxygenated monoterpene	terpinene-4-ol	1171	1165	0.13 ± 0.0
Phenylpropenes	estragol	1187	1175	2.40 ± 0.0
Oxygenated monoterpene	α-phellandrene epoxide	1195	1175	0.18 ± 0.0
Phenylpropenes	*p*-anisaldehyde	1234	1224	0.51 ± 0.0
Phenylpropenes	(Z)-anethole	1243	1257	0.21 ± 0.0
Phenylpropenes	(E)-anethole	1278	1269	40.58 ± 0.1
Phenylpropenes	Eugenol	1346	1330	1.03 ± 0.0
Sesquiterpene	β-caryophyllene	1425	1420	0.19 ± 0.0
Sesquiterpene	α-bergamotene	1439	1436	0.15 ± 0.0
Phenylpropenes	foeniculin	1665	1677	0.46 ± 0.0
Monoterpene				**41.37 ± 0.01**
Oxygenated monoterpene				**10.92 ± 0.0**
Sesquiterpene				**0.34 ± 0.0**
Phenylpropenes				**45.19 ± 0.1**
Total				**97.82 ± 0.1**

Table S7: Chemical composition of anise essential oil (n=3).

Class	Constituents	RI calc. HP-1	RI litt. HP-1	% ± SD
Monoterpene	α-pinene	934	932	0.57 ± 0.0
Monoterpene	sabinene	971	968	0.04 ± 0.0
Monoterpene	β-pinene	975	972	0.14 ± 0.0
Monoterpene	myrcene	989	983	0.08 ± 0.0
Monoterpene	α-phellandrene	1002	1020	0.29 ± 0.0
Monoterpene	δ-3-carene	1010	1006	0.16 ± 0.0
Monoterpene	*p*-cymene	1014	1014	0.04 ± 0.0
Monoterpene	*m*-cymene	1018	1027	0.10 ± 0.0
Monoterpene	β-phellandrene	1025	1021	0.32 ± 0.0
Monoterpene	limonene	1026	1024	1.13 ± 0.0
Monoterpene	γ-terpinene	1055	1051	0.16 ± 0.0
Monoterpene	terpinolene	1085	1080	0.05 ± 0.0
Oxygenated monoterpene	linalol	1094	1086	1.84 ± 0.0
Oxygenated monoterpene	camphor	1130	1123	0.03 ± 0.0
Oxygenated monoterpene	terpinene-4-ol	1171	1165	0.14 ± 0.0
Oxygenated monoterpene	α-terpineol	1184	1175	0.11± 0.0
Phenylpropenes	estragol	1187	1175	3.88 ± 0.0
Phenylpropenes	*p*-anisaldehyde	1235	1224	0.52 ± 0.0
Phenylpropenes	(Z)-anethole	1243	1257	0.23 ± 0.0
Phenylpropenes	(E)-anethole	1281	1269	86.54 ± 0.2
Sesquiterpene	α-copaene	1382	1374	0.05 ± 0.0
Sesquiterpene	unknown 1	1419	/	0.05 ± 0.0
Sesquiterpene	β-caryophyllene	1425	1420	0.30 ± 0.0
Sesquiterpene	α-bergamotene	1439	1436	0.32 ± 0.0
Sesquiterpene	β-farnesene	1454	1457	0.02 ± 0.0
Sesquiterpene	α-farnesene	1503	1497	0.05 ± 0.0
Sesquiterpene	α-bisabolene	1508	1494	0.06 ± 0.0
Sesquiterpene	γ-muurolene	1515	1473	0.01 ± 0.0
Sesquiterpene	δ-cadinene	1524	1516	0.05 ± 0.0
Oxygenated sesquiterpene	(E)-nerolidol	1558	1550	0.06 ± 0.0
Oxygenated sesquiterpene	T-muurolol	1654	1628	0.06 ± 0.0
Phenylpropene	foeniculin	1666	1677	1.06 ± 0.0
Monoterpene				**3.08 ± 0.0**
Oxygenated monoterpene				**2.12 ± 0.0**
Sesquiterpene				**0.91 ± 0.0**
Oxygenated sesquiterpene				**0.12 ± 0.0**
Phenylpropene				**91.93 ± 0.21**
Total				**98.16 ± 0.21**

Table S8. Nano-emulsion characteristics according to essential oil (EO), surfactant and sonication treatment used. All the parameters are mean ± standard error (SE) of three replicates (n=3).
Z-Average=droplet size; PDI=PolyDispersion Index; ZP= droplet surface charge (ζ-potential).

EO	Surfactant	Sonication	Z-Average ± SE (nm)	PdI ± SE	ZP ± SE (mV)
Anise	Span 20	No	5268 ± 312	0.25 ± 0.09	-53.27 ± 1.18
		Yes	265 ± 8	0.28 ± 0.01	-43.63 ± 0.43
	Tween 20	No	6028 ± 345	0.35 ± 0.00	-30.70 ± 0.46
		Yes	180 ± 1	0.14 ± 0.01	-29.50 ± 0.72
	Tween 80	No	6361 ± 152	0.25 ± 0.03	-20.00 ± 0.38
		Yes	141 ± 1	0.17 ± 0.01	-20.57 ± 0.14
Artemisia	Span 20	No	2562 ± 186	0.78 ± 0.11	-55.63 ± 0.73
		Yes	257 ± 1	0.36 ± 0.01	-49.67 ± 0.32
	Span 80	No	701 ± 23	0.69 ± 0.02	-56.43 ± 2.33
		Yes	442 ± 2	0.57 ± 0.06	-53.60 ± 0.84
	Tween 20	No	362 ± 21	0.78 ± 0.08	-20.57 ± 0.12
		Yes	139 ± 1	0.29 ± 0.02	-17.67 ± 0.79
	Tween 80	No	199 ± 2	0.42 ± 0.02	-12.27 ± 0.26
		Yes	116 ± 2	0.19 ± 0.00	-10.60 ± 0.15
Fennel	Span 20	No	5444 ± 323	0.73 ± 0.02	-59.43 ± 1.45
		Yes	308 ± 9	0.33 ± 0.02	-50.77 ± 0.53
	Tween 20	No	245 ± 10	0.42 ± 0.03	-28.60 ± 1.08
		Yes	131 ± 1	0.16 ± 0.01	-29.60 ± 0.49
	Tween 80	No	321 ± 12	0.86 ± 0.03	-25.77 ± 0.35
		Yes	132 ± 1	0.15 ± 0.01	-26.77 ± 0.13
Lavander	Span 20	No	3403 ± 261	0.73 ± 0.13	-53.77 ± 1.15
		Yes	290 ± 4	0.34 ± 0.02	-44.17 ± 0.18
	Span 80	No	4785 ± 234	0.62 ± 0.17	-60.20 ± 2.29
		Yes	435 ± 4	0.50 ± 0.01	-51.87 ± 1.03
	Tween 20	No	1186 ± 80	0.68 ± 0.16	-20.07 ± 0.32
		Yes	182 ± 1	0.19 ± 0.01	-17.97 ± 0.37
	Tween 80	No	187 ± 2	0.38 ± 0.01	-15.13 ± 0.48
		Yes	146 ± 1	0.18 ± 0.01	-18.70 ± 0.17
Mint	Span 20	No	1678 ± 65	0.98 ± 0.02	-17.73 ± 0.34
		Yes	241 ± 2	0.24 ± 0.01	-49.03 ± 0.33

	Span 80	No	2728 ± 336	0.87 ± 0.02	-19.70 ± 0.70
		Yes	275 ± 1	0.29 ± 0.02	-53.63 ± 0.53
	Tween 20	No	1634 ± 114	1.00 ± 0.00	-30.33 ± 1.71
		Yes	306 ± 2	0.27 ± 0.01	-51.50 ± 0.06
	Tween 80	No	175 ± 2	0.37 ± 0.02	-22.43 ± 0.13
		Yes	149 ± 1	0.16 ± 0.01	-19.27 ± 0.41
Rosemary	Span 20	No	2730 ± 179	1.00 ± 0.00	-60.80 ± 1.54
		Yes	180 ± 1	0.15 ± 0.01	-43.07 ± 0.48
	Span 80	No	610 ± 29	0.66 ± 0.02	-74.17 ± 2.54
		Yes	354 ± 3	0.42 ± 0.01	-44.07 ± 0.20
	Tween 20	No	234 ± 2	0.37 ± 0.02	-27.07 ± 0.24
		Yes	212 ± 1	0.24 ± 0.01	-23.13 ± 0.22
	Tween 80	No	217 ± 1	0.36 ± 0.01	-18.63 ± 0.14
		Yes	146 ± 1	0.17 ± 0.01	-26.37 ± 0.20
Sage	Span 20	No	5044 ± 376	0.56 ± 0.08	-60.73 ± 0.55
		Yes	242 ± 1	0.30 ± 0.01	-44.43 ± 0.89
	Span 80	No	5072 ± 79	0.52 ± 0.04	-58.13 ± 2.19
		Yes	307 ± 4	0.36 ± 0.01	-50.63 ± 0.55
	Tween 20	No	292 ± 2	0.53 ± 0.01	-23.93 ± 0.49
		Yes	195 ± 1	0.24 ± 0.01	-18.70 ± 0.15
	Tween 80	No	246 ± 1	0.49 ± 0.02	-20.70 ± 0.43
		Yes	188 ± 2	0.20 ± 0.01	-20.57 ± 0.29